THE JOURNAL OF BIOLOGICAL CHEMISTRY VOL. 285, NO. 36, pp. 28126–28133, September 3, 2010

Role of NEK6 in Tumor Promoter-induced Transformation in JB6 C141 Mouse Skin Epidermal Cells*[S]

Received for publication, April 22, 2010, and in revised form, June 30, 2010 Published, JBC Papers in Press, July 1, 2010, DOI 10.1074/jbc.M110.137190

Young Jin Jeon[‡§1], Kun Yeong Lee[‡1], Yong-Yeon Cho[‡], Angelo Pugliese[‡], Hong Gyum Kim[‡], Chul-Ho Jeong[‡], Ann M. Bode[‡], and Zigang Dong[‡2]

From [‡]The Hormel Institute, University of Minnesota, Austin, Minnesota 55912 and the [§]College of Medicine, Chosun University, 375 Susukdong, Kwangju 501-709, Korea

NEK6 (NIMA-related kinase 6) is a homologue of the *Aspergillus nidulans* protein NIMA (never in mitosis, gene A). We demonstrate that overexpression of NEK6 induces anchorage-independent transformation of JB6 Cl41 mouse epidermal cells. Tissue arrays and Western immunoblot analysis show that NEK6 is overexpressed in malignant tissues and several cancer cell lines. Our data also show that NEK6 interacts with STAT3, an oncogenic transcription factor, and phosphorylates STAT3 on Ser^{727}, which is important for transcriptional activation. Additional studies using NEK6 mutants suggested that the phosphorylation on both Ser^{206} and Thr^{210} of NEK6 is critical for STAT3 phosphorylation and anchorage-independent transformation of mouse epidermal cells. Notably, knockdown of NEK6 decreased colony formation and STAT3 Ser^{727} phosphorylation. Based on our findings, the most likely mechanism that can account for this biological effect involves the activation of STAT3 through the phosphorylation on Ser^{727}. Because of the critical role that STAT3 plays in mediating oncogenesis, the stimulatory effects of NEK6 on STAT3 and cell transformation suggest that this family of serine/threonine kinases might represent a novel chemotherapeutic target.

NEK6 (NIMA-related kinase 6) is a serine/threonine kinase identified as a homologue of the *Aspergillus nidulans* protein NIMA (never in mitosis, gene A). *Aspergillus* NIMA is essential for the initiation of mitosis, and its degradation is necessary for mitotic exit (1, 2). The NEK6 protein level is also increased during mitosis, concomitant with an increase in NEK6 activity (3). Overexpression of catalytically inactive NEK6 causes arrest of cells in mitosis and interferes with chromosome segregation (4). Furthermore, depletion of the endogenous NEK6 protein using siRNA in HeLa cells resulted in mitotic arrest followed by apoptosis (4). Therefore, NEK6 activity appears to be required for proper anaphase progression with cells either arresting at the spindle checkpoint and undergoing apoptosis or completing mitosis but with the acquisition of nuclear abnormalities in the process. Inhibition of NEK6 has been suggested to be involved in G_2/M phase cell cycle arrest induced by DNA damage (5).

Despite the critical role of NEK6 in maintaining proper progression of the cell cycle, the physiological substrates of NEK6 are largely undefined. NEK6 was initially identified in a screen to determine upstream kinases of the 70 ribosomal S6 kinase (6). However, additional evidence did not support S6 kinase as a physiological substrate of NEK6 (7). NEK6 was suggested to phosphorylate the kinesin Eg5 at a novel site necessary for mitotic spindle formation (8).

A possible role for NEK6 in tumorigenesis has been indicated. Analysis of hepatic cancer carcinomas showed that *nek6* mRNA expression was up-regulated in 70% of all cancers examined and correlated well with the up-regulation of peptidyl-prolyl isomerase or Pin1 (9). Because Pin1 plays an important role in the regulation of cell cycle and is prevalently overexpressed in human cancers, it is regarded as a new potential therapeutic target. Furthermore, evidence indicates that the growth rate of MDA-MB-231 human breast cancer cells is reduced by the overexpression of catalytically inactive NEK6 (4). However, the biological functions and mechanisms of NEK6 activity in carcinogenesis are largely unknown. Thus, the identification of key substrates is probably the most important component in discovering the function of NEK6 in carcinogenesis.

In the present study, we demonstrate that NEK6 is overexpressed in various human cancer tissues, and ectopic expression of NEK6 increases tumor promoter-induced transformation of JB6 Cl41 mouse epidermal cells. We also discovered that STAT3, a member of the signal transducers and activators of transcription (STAT) family, is a novel target of NEK6. STAT3, which was originally discovered as a mediator in the cytokine signaling pathway, plays an important role in carcinogenesis, including anchorage-independent transformation of JB6 Cl41 cells (10). Taken together, these results provide strong evidence linking NEK6 to carcinogenesis.

MATERIALS AND METHODS

Reagents and Antibodies—The pcDNA4/HisMaxC plasmid used for the construction of the expression vector was from Invitrogen (Carlsbad, CA). Short hairpin RNA for NEK6 was purchased from Open Biosystems (Huntsville, AL). Cell culture medium and other supplements were purchased from Invitrogen. Antibodies specific for NEK6 and Xpress were purchased from Abcam (Cambridge, MA) and Invitrogen, respectively. The antibody specific for pNEK6 (Ser^{206}) was raised in rabbits and affinity-purified. Antibodies to detect VP16, GAL4-HRP,

* This work was supported, in whole or in part, by National Institutes of Health Grants CA077646, R37CA081064, CA111536, CA120388, and ES016548. This work was also supported by the Hormel Foundation.

[S] The on-line version of this article (available at http://www.jbc.org) contains supplemental Figs. 1–6.

[1] Both authors contributed equally to this work.

[2] To whom correspondence should be addressed: The Hormel Institute, University of Minnesota, 801 16th Ave. NE, Austin, MN 55912. Tel.: 507-437-9600; Fax: 507-437-9606; E-mail: zgdong@hi.umn.edu.

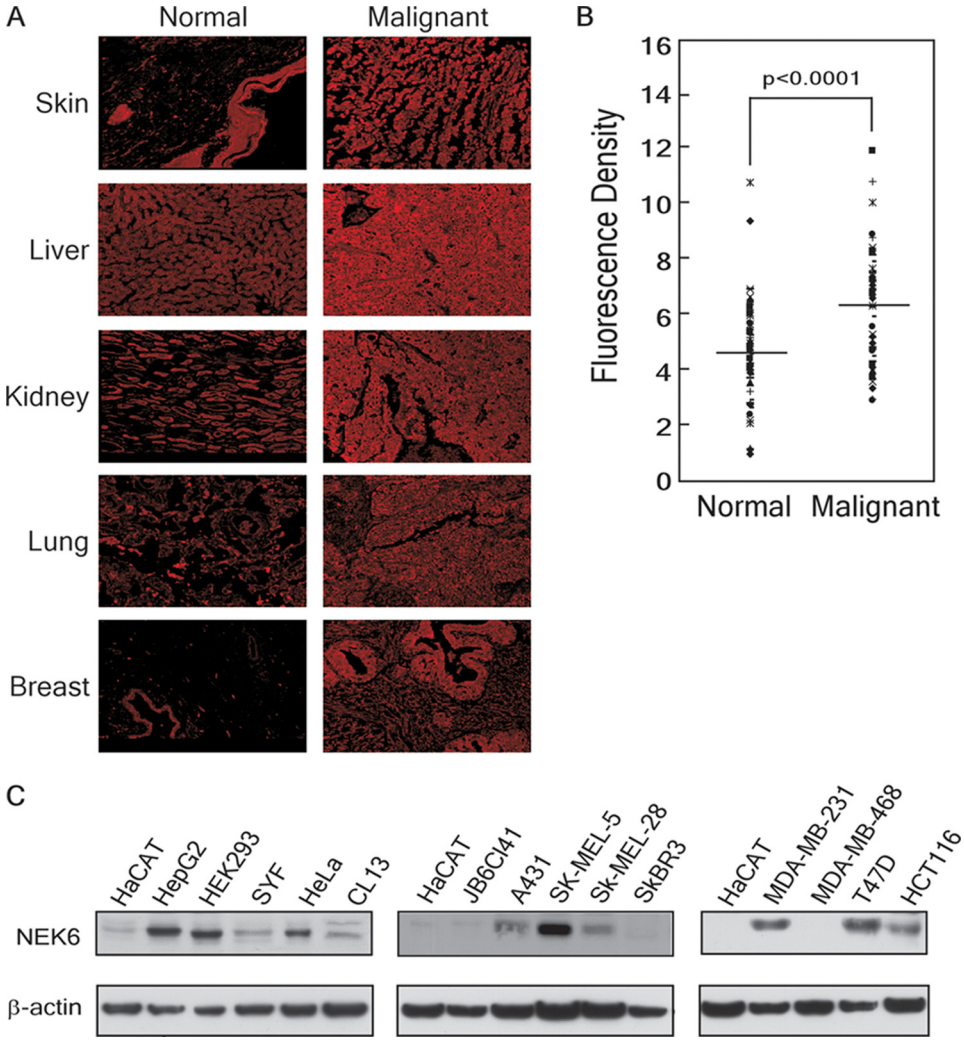

FIGURE 1. **NEK6 is overexpressed in malignant cancer tissues.** *A*, immunofluorescence staining of a human cancer tissue array, which included 47 tumors from multiple organ sites and matched normal tissues, was carried out as described under "Materials and Methods." Five representative tissues were selected, and the NEK6 protein abundance in cancer tissues was compared with matched normal tissues. *B*, analysis of average density of normal and cancer tissues. The light intensity was assessed using the Image J computer program. The individual density distribution of each normal and cancer tissue is denoted, and the average density of cancer and normal tissues is presented as a *horizontal bar* in the *graph*. *C*, differential expression of NEK6 in normal and cancer cell lines. Proteins were isolated from different cell lines, and the expression of NEK6 was analyzed by Western blot. β-Actin served as a loading control.

cyclin D1, c-Myc, α-tubulin, and lamin B were from Santa Cruz Biotechnology, Inc. (Santa Cruz, CA). Antibodies against STAT3, phospho-STAT3 (Ser^{727}), phospho-STAT3 (Tyr^{705}), and phosphothreonine were from Cell Signaling Technology, Inc. (Beverly, MA). Antibodies against β-actin was from Sigma. His-NEK6 and GST-STAT3 fusion proteins were purchased from Upstate Biotechnologies (Millipore, Chelmsford, MA) and Signal Chem (Richmond, Canada), respectively.

Construction of Vectors—The cDNA of each transcription factor was amplified by PCR and then introduced into the pACT mammalian two-hybrid system vector (pACT-TF) (11). We introduced NEK6 cDNA into the EcoRI/NotI site of the pBIND mammalian two-hybrid system vector (pBIND-NEK6) as bait. The NEK6 coding fragment from pBIND-NEK6 was introduced into pcDNA4-HisMaxC. Mutants NEK6 K74M/K75M, T202A, S206A, and T210A were constructed by using Site-directed Mutagenesis Kit II (Stratagene, La Jolla, CA). The constructed expression vectors were confirmed by restriction mapping and DNA sequencing.

Cell Culture and Transfections—JB6 Cl41 mouse skin epidermal cells were cultured in minimum Eagle's medium supplemented with 5% fetal bovine serum (FBS) and antibiotics at 37 °C in a 5% CO_2 incubator. HEK293 and HeLa cells were cultured with minimum Eagle's medium and DMEM supplemented with 10% FBS. For transfection experiments, cells were split, and the expression vectors were introduced using jetPEI (Qbiogen, Inc., Montreal, Canada) following the manufacturer's suggested protocol when cells reached 50–60% confluence.

Tissue Array—A multiple-cancer tissue array (MC962) was purchased from Biomax (US Biomax Inc., Rockville, MD) and utilized according to the manufacturer's suggested protocols. The slide was baked at 60 °C for 2 h, deparafinized, and rehydrated. Antigens were then unmasked by submerging the slide into boiling sodium citrate buffer (10 mM, pH 6.0) for 10 min. The sample was blocked with 3% BSA in 1× PBS, 0.03% Triton X-100 in a humidified chamber for 1 h at room temperature and incubated with a NEK6 antibody (1:200 dilution in 1× PBS, 0.03% Triton X-100) at 4 °C in the humidified chamber overnight. The slide was washed and hybridized with a secondary antibody (donkey anti-rabbit) conjugated with Cy3 (1:1000) for 1.5 h at room temperature in the dark. The tissue array was then washed and mounted with GEL/MOUNT solution containing anti-fading agents, and the array slide was observed by laser-scanning confocal microscopy (NIKON $C1^{si}$ confocal spectral imaging system) using a CFI Plan Fluor ×20 objective.

Western Blotting—Samples containing equal amounts of protein were resolved by the appropriate percentage SDS-PAGE and transferred onto polyvinylidene difluoride membranes. The membranes were incubated in blocking buffer and then probed with specific primary antibodies against appropriate proteins as indicated. The Western blots were visualized using an enhanced chemiluminescence detection system (Amersham Biosciences).

Anchorage-independent Cell Transformation Assay—EGF- or TPA-induced cell transformation was investigated in mock or pcDNA4-NEK6 stably transfected cells. In brief, cells (8 ×

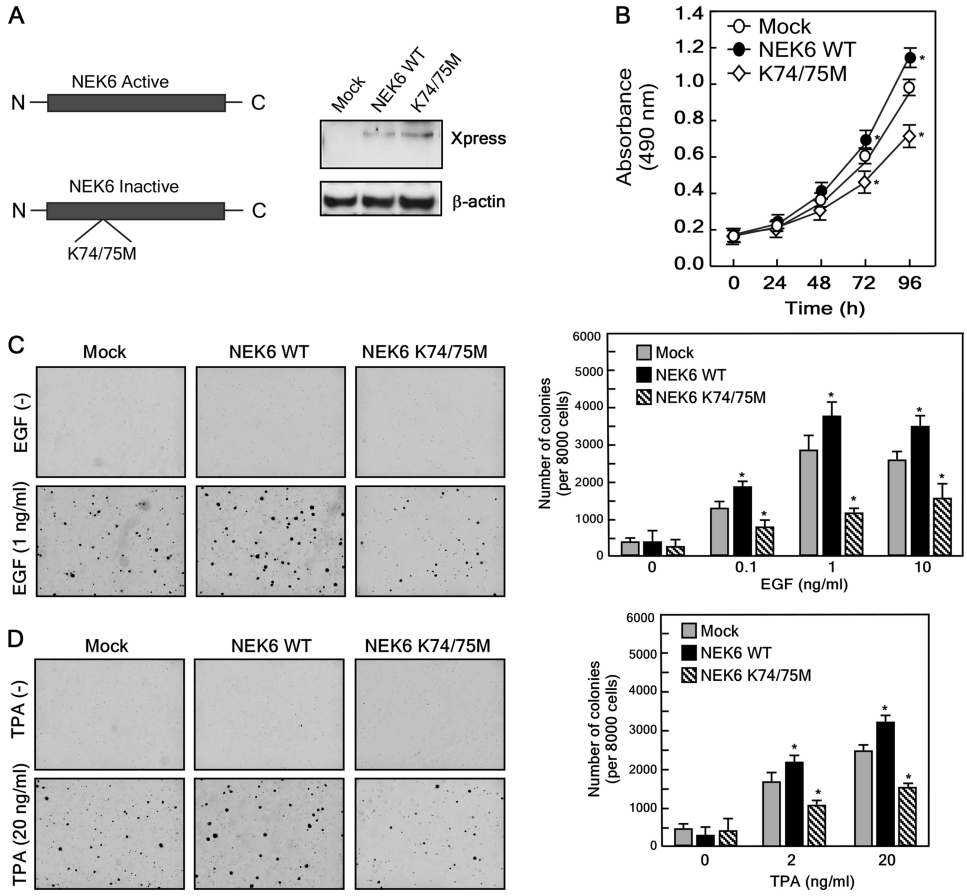

FIGURE 2. **NEK6 protein expression increases anchorage-independent cell transformation in tumor promoter-stimulated JB6 Cl41 cells.** *A*, stable transfectants of JB6 Cl41 cells expressing mock (*pcDNA4-mock*), wild type (*pcDNA4-NEK6*), or mutant (*pcDNA4-NEK6 K74M/K75M*) NEK6 were established, and overexpression was confirmed by Western blot using an antibody to detect the Xpress tag. *B*, NEK6 wild type cells grow significantly faster than mock or mutant cells. Cells were seeded (1×10^3/well) into 96-well plates in 5% FBS-DMEM, and proliferation was estimated by a Cell Titer 96 AQueous (MTS) assay. *C* and *D*, NEK6 expression increases EGF-induced (*C*) or TPA-induced (*D*) anchorage-independent cell transformation. Representative microphotographs are shown (*left*), and data are presented (*right*) as means ± S.D. (*error bars*) of triplicate determinations. *, a response that is significantly different from the control group as determined by Student's two-tailed *t* test ($p < 0.05$).

10^3/ml) were exposed to EGF (0.1–10 ng/ml) or TPA[3] (2–20 ng/ml) in 1 ml of 0.3% basal medium Eagle agar containing 10% FBS. The cultures were maintained in a 37 °C, 5% CO_2 incubator for 10 days (EGF) or 3–4 weeks (TPA), and the cell colonies were scored using a microscope and the Image-Pro PLUS (*version* 4) computer software program (Media Cybernetics, Silver Spring, MD) as described by Colburn *et al.* (12).

Mammalian Two-hybrid Assay—HEK293 cells (2.0×10^4) were seeded into 48-well plates and incubated with 10% FBS-DMEM for 18 h before transfection. The plasmids expressing pACT transcription factors, pBIND-NEK6, and pG5 luciferase reporter plasmid were combined in the same molar ratio and transfected. The cells were disrupted by the addition of cell lysis buffer directly into each well of the 48-well plate, and then aliquots of 40 μl were added to each well of a 96-well luminescence plate. The relative luciferase activity was calculated and normalized based on the pG5-luciferase basal control. For assessment of transfection efficiency and protein amount, the luciferase assay and the *Renilla* luciferase activity assay were used.

In Vitro Kinase Assay—The GST-STAT3 protein was used for an *in vitro* kinase assay with active NEK6. Reactions were carried out at 30 °C for 30 min in a mixture containing 50 μM unlabeled ATP and 10 μCi of [γ-^{32}P]ATP and then stopped by adding 6× SDS sample buffer. Samples were boiled, separated by 12% SDS-PAGE, and visualized by autoradiography, Western blotting, or Coomassie Blue staining.

Homology Modeling of NEK6—A spatial structural model of active NEK6 was constructed and optimized with the program Prime version 2.1 (Schrödinger, LLC, New York) based on the sequence alignment with the known crystal structure of active MAP3K TAO2 kinase (Protein Data Bank code 2GCD). The sequence identities and similarities between the template (TAO2) and the target (NEK6) were 32 and 51%, respectively. The activation loop, comprising Thr^{202}, Ser^{206}, and Thr^{210}, was phosphorylated, and the model was further refined with 1.2 ns of molecular dynamics in explicit solvent using the program Desmond (Schrödinger, LLC, New York). The final model was analyzed with the Molprobity web service (15) for structural inconsistencies. Ramachandran analysis (16) showed that 86.4% of all residues were in favored (98%) regions and that 97.9% were in allowed regions (>99.8%), suggesting a reliable molecular arrangement.

RESULTS

The NEK6 Protein Abundance Is Increased in Malignant Cancer Tissues and Various Cancer Cell Lines—To investigate the role of NEK6 in carcinogenesis, we compared the abundance of NEK6 in cancer and normal tissues. Immunofluorescence staining of 47 matched pairs of normal and cancer tissues showed that NEK6 is overexpressed in cancer tissues compared with normal tissues (Fig. 1*A*). Densitometric analysis of each matched sample indicated that 77% of the cancer tissues exhibited increased NEK6 protein levels compared with normal control tissue samples (data not shown). The average total fluorescence density of all cancer tissues was 1.4-fold higher ($p < 0.001$) than the average density of matched normal tissues (Fig. 1*B*).

To further examine whether NEK6 is overexpressed in cancer cells, we cultured several different malignant human cancer cell lines and non-malignant human and mouse cell lines. The

[3] The abbreviation used is: TPA, 12-*O*-tetradecanoylphorbol-13-acetate.

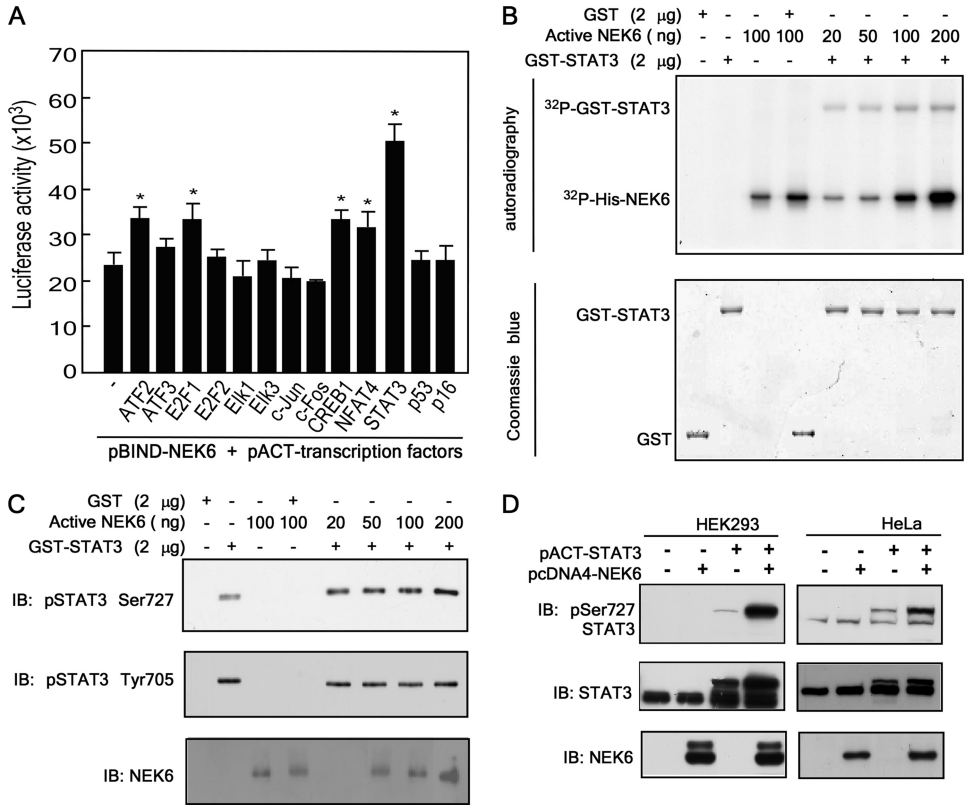

FIGURE 3. **NEK6 interacts with and phosphorylates STAT3.** *A*, NEK6 protein binding with various transcription factors was determined by the mammalian two-hybrid system. The individual pACT transcription factors were each co-transfected with pBIND-NEK6 and a pG5-luciferase reporter plasmid into HEK293 cells. Cells were subsequently analyzed for firefly luciferase activity. *B*, GST-STAT3 and active NEK6 were incubated with 10 μCi of [γ-^{32}P]ATP at 30 °C for 30 min. NEK6 phosphorylation of STAT3 was analyzed by autoradiography. *C*, GST-STAT3 and active NEK6 were incubated with 50 μM unlabeled ATP at 30 °C for 30 min. STAT3 phosphorylation was analyzed by Western blot (*IB*). *D*, pBIND-NEK6 and/or pACT-STAT3 were transfected into HEK293 and HeLa cells, and STAT3 Ser^{727} phosphorylation by NEK6 was determined by Western blot. *Error bars*, S.D.

NEK6 protein level was visualized by Western blot. The results indicated that many cancer cell lines, including HepG2, HeLa, SK-MEL-5, SK-MEL-28, MDA-MB-231, T47D, and HCT-116, showed higher NEK6 abundance compared with non-malignant human and mouse cell lines, such as HaCaT and JB6 Cl41 cells (Fig. 1*C*). Taken together, these results demonstrated that NEK6 is overexpressed in cancer tissues and cells and thus might play an important role in tumorigenesis.

Ectopic Expression of NEK6 Induces Anchorage-independent Cell Transformation—To investigate the role of NEK6 in tumor promotion, we established JB6 Cl41 cells stably expressing NEK6 wild type (WT) or a kinase-inactive mutant (K74M/K75M) (Fig. 2*A*). NEK6 expression in JB6 Cl41 cells increased proliferation, whereas kinase-inactive K74M/K75M decreased proliferation (Fig. 2*B*). Mock, NEK6 WT, or NEK6 K74M/K75M stable cell lines were subjected to a soft agar assay with stimulation by EGF (0, 0.1, 1, or 10 ng/ml) or TPA (0, 2, or 20 ng/ml) to assess transformation ability. Treatment of cells with EGF or TPA increased anchorage-independent colony formation in a dose-dependent manner (Fig. 2, *C* and *D*). JB6 Cl41 cells overexpressing NEK6 showed an increase in either EGF- or TPA-induced colony formation compared with mock control, whereas NEK6 K74M/K75M decreased EGF-induced (Fig. 2*C*) or TPA-induced transformation (Fig. 2*D*). These results demonstrate that NEK6 activity is important for transformation in tumor promoter-stimulated mouse epidermal cells.

NEK6 Interacts with and Phosphorylates STAT3—We investigated the interaction between NEK6 and several transcription factors known to be important in tumorigenesis. The selected transcription factors included ATF2 (17), ATF3 (18), E2F2 (19), Elk1 (20), Elk3 (21), c-Jun and c-Fos (22), CREB1 and NFAT4 (23), and STAT3 (10). We also selected two important tumor suppressors, p53 and p16, for examination. The cDNA of each transcription factor or tumor suppressor was amplified by PCR and then introduced into the pACT mammalian two-hybrid system vector (pACT-TF) (11). We introduced NEK6 cDNA into the pBIND mammalian two-hybrid system vector (pBIND-NEK6) as bait. Each individual pACT-TF and the pG5-luciferase reporter plasmid were co-transfected into HEK293 cells with pBIND-NEK6. Each interaction activity was compared against the activity of pG5-luciferase/pBIND-NEK6 as the basal level (Fig. 3*A*). Among the transcription factors and tumor suppressors, STAT3 showed a very strong interaction with pBIND-NEK6. We further examined the NEK6 interaction with other STATs using the mammalian two-hybrid assay and found that NEK6 most strongly interacts with STAT3 (supplemental Fig. 1). STAT3 is a well known oncogenic transcription factor and is involved in neoplastic transformation of mouse skin cells (10). Therefore, we focused on the interaction of NEK6 and STAT3. pBIND-NEK6 and pACT-STAT3 were co-transfected into HEK293 cells, and pACT-STAT3 was immunoprecipitated with anti-VP16. Results indicated that pBIND-NEK6 was co-precipitated with pACT-STAT3 (supplemental Fig. 2*A*). Transfection and immunoprecipitation of NEK6 further confirmed that NEK6 interacts with endogenous STAT3 (supplemental Fig. 2*B*). Immunofluorescence staining of HeLa with antibodies against pNEK6 (Ser^{206}) and pSTAT3 (Ser^{727}) showed the co-localization of NEK6 and STAT3 (supplemental Fig. 3).

To determine whether this interaction induced STAT3 phosphorylation, we performed an *in vitro* kinase assay. Incubation of a GST-STAT3 fusion protein with active NEK6 in the presence of [γ-^{32}P]ATP showed that STAT3 was strongly phosphorylated by NEK6 in a dose-related manner (Fig. 3*B*). These results demonstrate that NEK6 interacts with and phosphorylates STAT3, an event that could play an important role in oncogenesis. For the maximal activation of

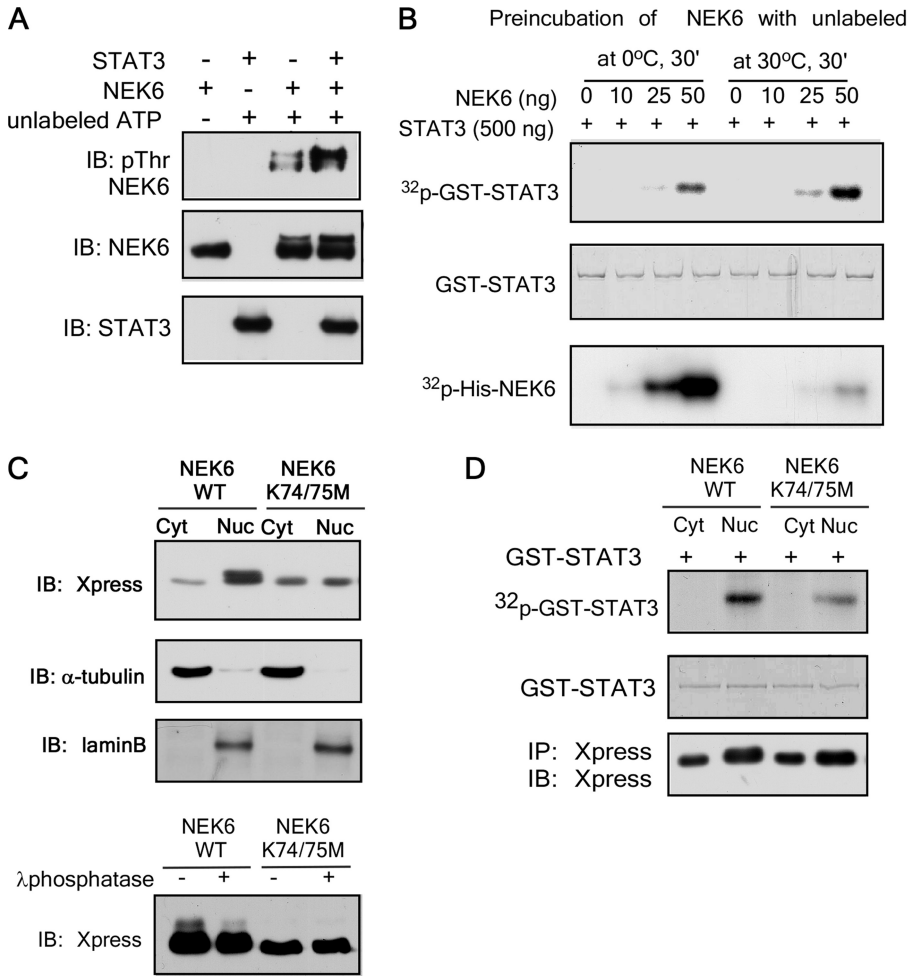

FIGURE 4. **NEK6 autophosphorylation increases its kinase activity.** *A*, GST-STAT3 and active NEK6 were incubated with ATP at 30 °C for 30 min. NEK6 autophosphorylation was detected with a phosphothreonine antibody. *B*, NEK6 was preincubated with unlabeled ATP at 0 or 30 °C for 30 min and then incubated with GST-STAT3 and 10 μCi of [γ-^{32}P]ATP at 30 °C for 15 min. NEK6 phosphorylation of STAT3 was analyzed by gel electrophoresis and autoradiography. *C*, NEK6 wild type and mutant K74M/K75M plasmids were each transfected into HEK293 cells. Cytosolic and nuclear extracts were prepared, and NEK6 protein localization was determined by Western blot (*upper panels*). α-Tubulin and lamin B were detected to confirm the purity of cytosolic and nuclear fractions, respectively. Nuclear extracts isolated from the transfectants were treated with λ-phosphatase and subjected to Western blot (*lower panel*). *D*, the cytosolic and nuclear extracts were immunoprecipitated with anti-Xpress, and an *in vitro* kinase assay was conducted. *IB*, immunoblot; *IP*, immunoprecipitation.

demonstrate that NEK6 phosphorylates STAT3 both *in vitro* and *ex vivo*.

Autophosphorylation of NEK6 Increases Its Kinase Activity—The *in vitro* kinase assay showed that NEK6 has strong autophosphorylation activity (Fig. 3*B*). Moreover, transfection of HEK293 cells with pcDNA4-NEK6 produced an additional delayed or retarded NEK6 band (Fig. 3*D*). To determine whether this slower migration of NEK6 was due to threonine autophosphorylation, we performed Western blotting using antibodies against phosphothreonines. The phosphothreonine antibody detected two NEK6 bands resulting from the *in vitro* kinase assay with unlabeled ATP, whereas incubation of NEK6 without ATP showed no detectable threonine phosphorylation (Fig. 4*A*). This result demonstrates that possibly more than two amino acid residues of NEK6 are autophosphorylated by NEK6 itself. Notably, the threonine autophosphorylation was further increased in the presence of STAT3 (Fig. 4*A*).

To further analyze the relationship between autophosphorylation and enzyme activity of NEK6, we preincubated NEK6 with unlabeled ATP at 30 °C for 30 min to induce autophosphorylation and performed an *in vitro* kinase assay with STAT3 in the presence of [γ-^{32}P]ATP for 15 min. Preautophosphorylation of NEK6 (in the presence of unlabeled ATP) significantly increased STAT3 phosphorylation (Fig. 4*B*). These data suggest that autophosphorylation of NEK6 increases its kinase activity.

STAT3 signaling, phosphorylation of both Tyr^{705} and Ser^{727} is required. Phosphorylation of Tyr^{705} induces dimerization, nuclear translocation, and DNA binding of the STAT3 protein, whereas phosphorylation of Ser^{727} is important for transcriptional activation. Because NEK6 binds and phosphorylates STAT3, we used an *in vitro* kinase assay and Western blotting to determine whether this serine-threonine kinase can phosphorylate Ser^{727}. Incubation of active NEK6 and STAT3 in the presence of unlabeled ATP showed that NEK6 increased STAT3 phosphorylation at Ser^{727} (Fig. 3*C*).

To investigate whether NEK6 can phosphorylate STAT3 at Ser^{727} in a cell culture system, we transfected NEK6 and/or STAT3 into HEK293 and HeLa cells. Co-transfection of STAT3 with NEK6 substantially increased STAT3 phosphorylation of Ser^{727} in both HEK293 and HeLa cells (Fig. 3*D*). These results

We next transfected NEK6 wild type and the kinase-inactive mutant K74M/K75M each into HEK293 cells and isolated cytosolic and nuclear fractions to determine localization of NEK6. NEK6 localizes both in the cytosol and nucleus (Fig. 4*C*). Slow migrating NEK6 was detected mainly in the nucleus of the wild type NEK6-transfected cells. However, slow migrating NEK6 was not detectable in the mutant NEK6 K74M/K75M-transfected cells. To confirm that the band shift of NEK6 was dependent on phosphorylation, we treated the nuclear fraction isolated from wild type- or mutant-transfected cells with λ-phosphatase. Phosphatase substantially decreased the retarded band density in wild type NEK6-transfected cells (Fig. 4*C*, *bottom*). Although NEK6 is distributed in both

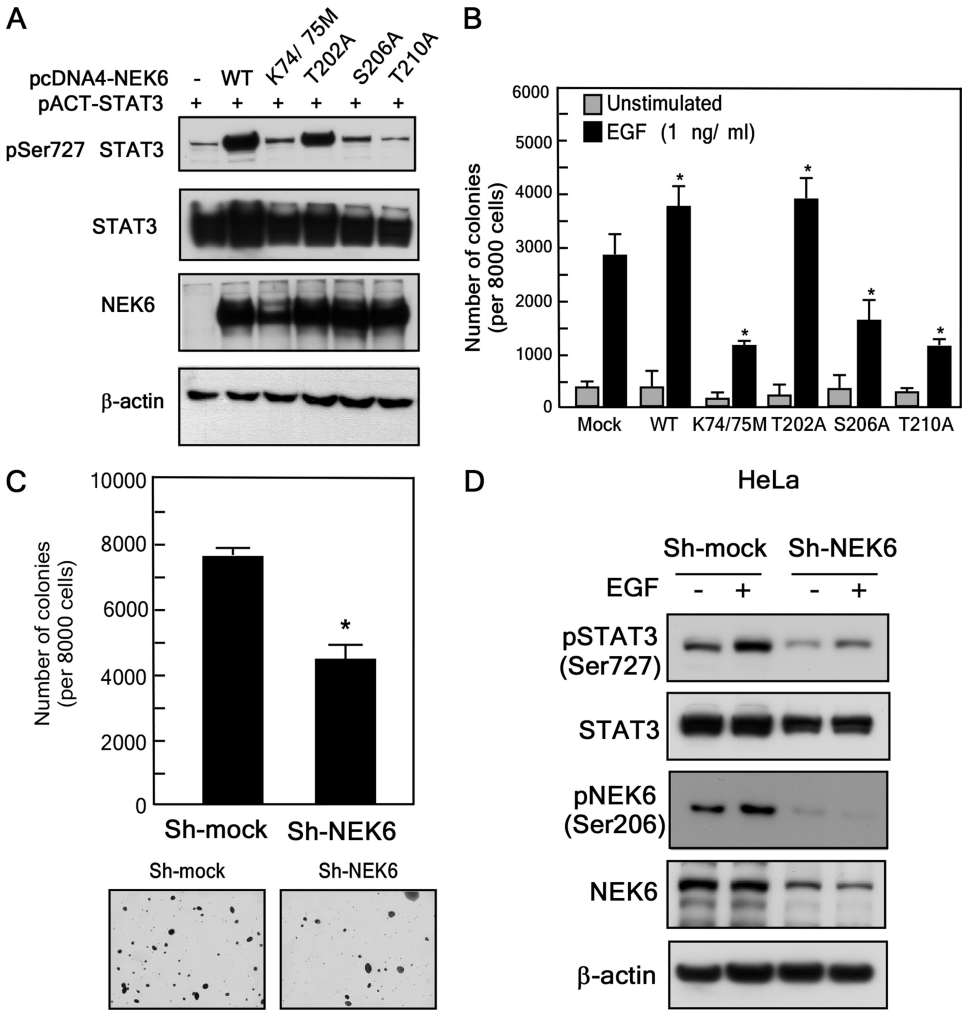

FIGURE 5. **Effects of ectopic expression of NEK6 mutants or knockdown of NEK6 on anchorage-independent cell growth.** *A*, NEK6 wild type or mutant K74M/K75M, T202A, S206A, and T210A were each transfected with pACT-STAT3 into HeLa cells, and STAT3 (Ser^{727}) phosphorylation was determined by Western blot. *B*, stable transfectants of JB6 Cl41 cells expressing mock, NEK6, K74M/K75M, T202A, S206A, or T210A were established and subjected to a soft agar assay. *C*, HeLa cells were infected with lentiviruses expressing short hairpin NEK6 and subjected to a soft agar assay. *D*, HeLa cells were infected with lentiviruses expressing short hairpin NEK6, treated with EGF (10 ng/ml), and subjected to Western blot. *Error bars*, S.D.

the cytosol and nucleus, the retarded NEK6 band was detected mainly in the nucleus. We transfected NEK6 wild type and the mutant K74M/K75M, respectively, into HEK293 cells. Results of the immunoprecipitation and *in vitro* kinase assay showed that NEK6 in the nuclear fraction has kinase activity (Fig. 4*D*). Taken together, these results demonstrate that autophosphorylation of NEK6 on threonine residues significantly increases the kinase activity and STAT3 phosphorylation.

Effects of NEK6 Mutants on EGF-induced Anchorage-independent Cell Transformation—Several amino acids in the activation loop of NEK6, including Thr^{202}, Ser^{206}, and Thr^{210}, have been suggested to be important for NEK6 kinase activity (3, 24). To investigate the role of these amino acids in the phosphorylation of STAT3, we constructed NEK6 T202A, S206A, and T210A mutants (supplemental Fig. 4) and transfected each individually into HeLa cells with pACT-STAT3. The effect on STAT3 Ser^{727} phosphorylation was then assessed. The wild type NEK6 and the T202A mutant exhibited increased STAT3 Ser^{727} phosphorylation compared with mock control. On the other hand, no increase in phosphorylation was observed in the K74M/K75M, S206A, or T210A mutant (Fig. 5*A*). We then established JB6 Cl41 cells that stably expressed NEK6 WT, K74M/K75M, T202A, S206A, or T210A. NEK6 and T202A expression in JB6 Cl41 cells increased proliferation, whereas K74M/K75M, S206A, and T210A decreased proliferation (supplemental Fig. 5). Overexpression of NEK6 or T202A increased EGF-induced colony formation compared with the mock control, whereas K74M/K75M, S206A, or T210A decreased EGF-induced cell transformation (Fig. 5*B*). These results demonstrate that NEK6 phosphorylation of STAT3 Ser^{727} corresponds well with transformation of tumor promoter-stimulated mouse epidermal cells.

NEK6 knockdown in HeLa cells decreased colony formation (Fig. 5*C*). We further analyzed the effect of NEK6 knockdown on the phosphorylation of STAT3 Ser^{727}. NEK6 knockdown in HeLa cells inhibited EGF-induced phosphorylation of STAT3 Ser^{727} (Fig. 5*D*) as well as STAT3-target gene expression (supplemental Fig. 6).

Homology Modeling of NEK6—We next performed a structural modeling experiment to shed light on the role of $Thr(P)^{202}$, $Ser(P)^{206}$, and $Thr(P)^{210}$ in binding with STAT3 and consequent Ser^{727} phosphorylation, leading to decreased cell transformation. The structural modeling was based on the available x-ray crystal structure of active MAP3K TAO2 kinase (Protein Data Bank code 2GCD) and was undertaken to determine the possible NEK6 molecular arrangement. The homology model suggests that the three phosphorylated amino acids in the activation loop might contribute to the stabilization of the active form of the protein due to favorable charge-charge interactions with positive charged residues located close by on the kinase domain (Fig. 6*A*). The configuration of the activation loop also suggests that only $Thr(P)^{210}$ and $Ser(P)^{206}$ may actively participate in the binding with STAT3 because of the marginal position of $Thr(P)^{202}$ relative to the ATP pocket vicinity (compared with $Thr(P)^{210}$ and $Ser(P)^{206}$), which might eliminate this residue from the region where binding surfaces (recruitment sites) for downstream signaling proteins are usually located (Fig. 6, *A* and *B*) (25).

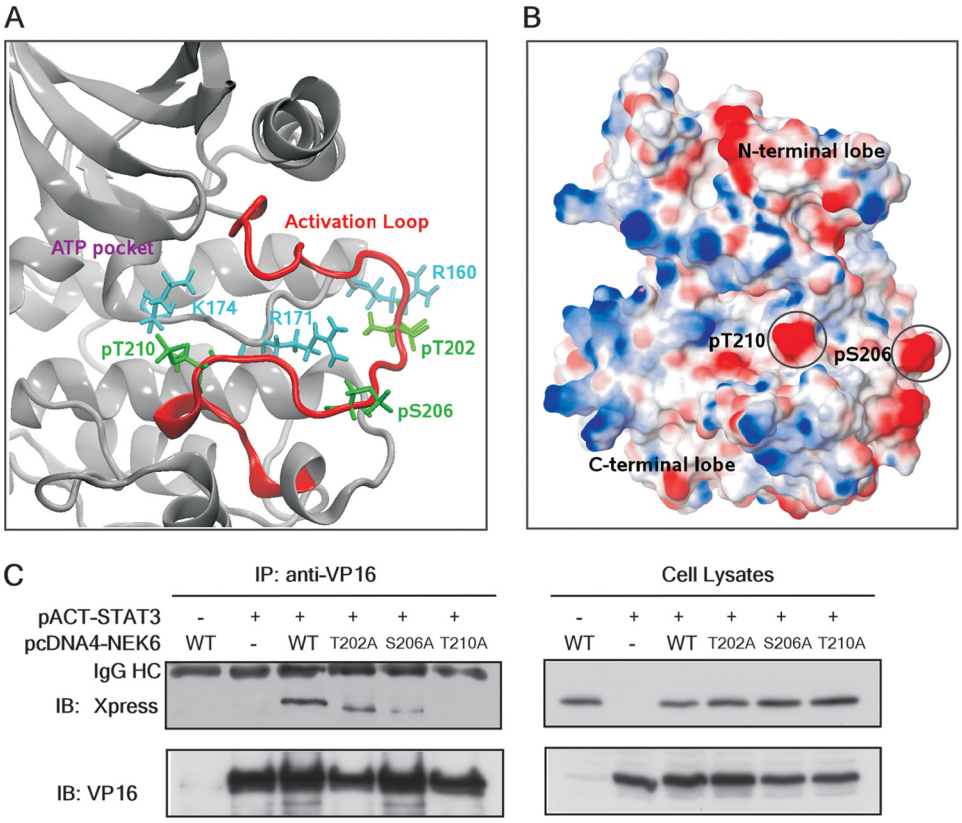

FIGURE 6. **Homology model of NEK6.** *A*, a magnified view of the NEK6 activation loop is depicted as a *red schematic diagram*, and the remaining protein is shown as a *gray schematic diagram*. Within the activation loop, the three phosphorylated residues are shown as *green sticks*, and the positive charged residues are shown as *light blue sticks*. *B*, electrostatic surface potential representation of the entire NEK6 homology model with the catalytic cleft between the two lobes facing up, highlighting the position of the negatively charged (*red*) phosphorylated threonine (Thr(P)^{210}; *pT210*) and serine (Ser(P)^{206}; *pS206*); the *blue color* represents positive charged regions on the surface of the protein. *C*, NEK6 wild type and mutants, T202A, S206A, and T210A, were each transfected with pACT-STAT3 into HEK293 cells, and the interaction was determined by immunoprecipitation (*IP*) and Western blot (*IB*).

To confirm the ideas raised by the homology model of NEK6, we compared the binding activity of NEK6 with that of mutants. NEK6 WT, T202A, S206A, and T210A were each transfected with pACT-STAT3 into HEK293 cells, and the interaction was examined by immunoprecipitation (Fig. 6*C*). Because pACT-STAT3 expresses VP16-tagged recombinant STAT3, we used anti-VP16 to immunoprecipitate and detect pACT-STAT3. Wild type NEK6 and mutant T202A interacted with STAT3, whereas the binding activity of S206A and T210A was strongly reduced. These results demonstrate that the phosphorylation of NEK6 on Ser^{206} and Thr^{210} is critical to both the kinase activity and substrate binding.

DISCUSSION

We demonstrated that ectopic expression of NEK6 increases tumor promoter-induced cell transformation and STAT3 phosphorylation at Ser^{727}. The major finding of the present study is that NEK6 plays an important role in oncogenesis. Using the JB6 Cl41 cell transformation model, we showed that ectopic expression of NEK6 significantly increases the anchorage-independent growth induced by EGF or TPA. The expression of kinase-inactive NEK6 further confirmed the important role of NEK6 in tumor promoter-induced cell transformation. The function of NEK6 in cancer cell growth was suggested by a previous report indicating that the growth rate of MDA-MB-231 human breast cancer cells was reduced by the overexpression of catalytically inactive NEK6 (4). Our data also confirmed that NEK6 wild type or mutant K74M/K75M expression in JB6 Cl41 cells increased or decreased cell proliferation, respectively (Fig. 2*B*). Moreover, immunofluorescence staining of 47 pairs of normal and cancer tissues showed that the NEK6 protein was highly abundant in cancer tissues compared with normal tissues (Fig. 1). Chen *et al.* (9) also demonstrated that NEK6 mRNA expression was up-regulated in 70% of hepatic carcinomas. These results highlight the potential of NEK6 as a novel target of chemotherapeutic and chemopreventive agents.

We also showed that STAT3, an oncogenic transcription factor, is a novel target of NEK6 and an important mediator of oncogenesis by NEK6. Several lines of experimental evidence support this contention. First, when we tested the interaction between NEK6 and several transcription factors that are important in tumorigenesis or tumor suppression, we found that STAT3 is a strong binding partner of NEK6. Second, we showed that NEK6 phosphorylated STAT3 in a dose-dependent manner. Third, knockdown of NEK6 decreased STAT3 phosphorylation. Finally, based on the mutant NEK6 study, NEK6-mediated STAT3 Ser^{727} phosphorylation corresponds well with JB6 Cl41 cell transformation.

STAT3 is a member of the STAT family of cytoplasmic transcription factors, which play critical roles in cytokine and growth factor signaling. Activated STAT3 induces transformation of NIH-3T3 cells and produces tumors in nude mice (13, 26). Constitutive activation of STAT3 is detected in many human malignancies, including prostate, lung, brain, breast, and squamous cell carcinomas. Persistent STAT3 activation promotes uncontrolled growth and survival through deregulation of gene expression, including cyclin D1, c-*myc*, *bcl-xL*, *mcl-1*, and survivin genes, and thereby contributes to oncogenesis. Because of the critical role of STAT3 in oncogenesis, the stimulatory effects of NEK6 on anchorage-independent transformation of JB6 Cl41 mouse skin cells most likely involve the activation of STAT3. This was further confirmed by a report showing that STAT3 plays an important role in carcinogenesis, including anchorage-independent transformation of JB6 Cl41 cells (10).

One of the major findings of the present study is that the phosphorylation on both Ser^{206} and Thr^{210} of NEK6 is critical for STAT3 phosphorylation and anchorage-independent transformation of mouse epidermal cells. The importance of Ser^{206} was previously described in that Nercc/NEK9 catalyzes the direct phosphorylation of prokaryotic recombinant NEK6 at Ser^{206} *in vitro*, concomitant with a 20–25-fold activation of NEK6 activity toward S6 kinase phosphorylation (3). Lee *et al.* (24) reported that Fe65 interacts with NEK6, down-regulates Thr^{210} phosphorylation, and induces apoptosis. However, kinases that can phosphorylate Thr^{210} have not been identified. Because the T210A mutant significantly decreased NEK6 activity, the identification of the upstream kinase is very important for the mechanistic study of NEK6 regulation. Interestingly, Thr^{210} is followed by a proline residue that can be recognized by Pin1. The interaction between NEK6 and Pin1 has been reported (9). Pin1 specifically recognizes a proline preceded by a phosphorylated serine or threonine residue (phospho-Ser/Thr-Pro motif) and catalyzes the cis-trans isomerization of the target peptidyl-prolyl bonds (14). The importance of Ser^{206} and Thr^{210} for NEK6 activity was further explained by the homology model of NEK6. Ser^{206} and Thr^{210} seemed to be located at crucial sites for interacting with phosphoamino acid-binding proteins. These substrate recruitment sites are normally shaped by the conformation adopted by the activation loop upon phosphorylation. In contrast, Thr^{202} is on the edge of the pocket and thus does not seem to be part of the substrate binding surface. Therefore, the phosphorylation of Ser^{206} and Thr^{210} might possibly play an important role in the binding of substrates.

In summary, these experiments demonstrate that ectopic expression of NEK6 induces anchorage-independent transformation of JB6 Cl41 mouse epidermal cells. Based on our findings, the most likely mechanism that can account for this biological effect involves, at least in part, the activation of STAT3 through its phosphorylation on Ser^{727}. Because of the critical role that STAT3 plays in mediating oncogenesis, the stimulatory effects of NEK6 on STAT3 and cell transformation suggest that this family of serine/threonine kinases may represent a novel chemotherapeutic target.

REFERENCES

1. Osmani, S. A., May, G. S., and Morris, N. R. (1987) *J. Cell Biol.* **104,** 1495–1504
2. Pu, R. T., and Osmani, S. A. (1995) *EMBO J.* **14,** 995–1003
3. Belham, C., Roig, J., Caldwell, J. A., Aoyama, Y., Kemp, B. E., Comb, M., and Avruch, J. (2003) *J. Biol. Chem.* **278,** 34897–34909
4. Yin, M. J., Shao, L., Voehringer, D., Smeal, T., and Jallal, B. (2003) *J. Biol. Chem.* **278,** 52454–52460
5. Lee, M. Y., Kim, H. J., Kim, M. A., Jee, H. J., Kim, A. J., Bae, Y. S., Park, J. I., Chung, J. H., and Yun, J. (2008) *Cell Cycle* **7,** 2705–2709
6. Belham, C., Comb, M. J., and Avruch, J. (2001) *Curr. Biol.* **11,** 1155–1167
7. Lizcano, J. M., Deak, M., Morrice, N., Kieloch, A., Hastie, C. J., Dong, L., Schutkowski, M., Reimer, U., and Alessi, D. R. (2002) *J. Biol. Chem.* **277,** 27839–27849
8. Rapley, J., Nicolàs, M., Groen, A., Regué, L., Bertran, M. T., Caelles, C., Avruch, J., and Roig, J. (2008) *J. Cell Sci.* **121,** 3912–3921
9. Chen, J., Li, L., Zhang, Y., Yang, H., Wei, Y., Zhang, L., Liu, X., and Yu, L. (2006) *Biochem. Biophys. Res. Commun.* **341,** 1059–1065
10. Yu, C. Y., Wang, L., Khaletskiy, A., Farrar, W. L., Larner, A., Colburn, N. H., and Li, J. J. (2002) *Oncogene* **21,** 3949–3960
11. Cho, Y. Y., He, Z., Zhang, Y., Choi, H. S., Zhu, F., Choi, B. Y., Kang, B. S., Ma, W. Y., Bode, A. M., and Dong, Z. (2005) *Cancer Res.* **65,** 3596–3603
12. Colburn, N. H., Wendel, E. J., and Abruzzo, G. (1981) *Proc. Natl. Acad. Sci. U.S.A.* **78,** 6912–6916
13. Bromberg, J. F., Wrzeszczynska, M. H., Devgan, G., Zhao, Y., Pestell, R. G., Albanese, C., and Darnell, J. E., Jr. (1999) *Cell* **98,** 295–303
14. Wulf, G., Finn, G., Suizu, F., and Lu, K. P. (2005) *Nat. Cell Biol.* **7,** 435–441
15. Davis, I. W., Leaver-Fay, A., Chen, V. B., Block, J. N., Kapral, G. J., Wang, X., Murray, L. W., Arendall, W. B., 3rd, Snoeyink, J., Richardson, J. S., and Richardson, D. C. (2007) *Nucleic Acids Res.* **35,** W375–W383
16. Ramachandran, G. N., Ramakrishnan, C., and Sasisekharan, V. (1963) *J. Mol. Biol.* **7,** 95–99
17. Vlahopoulos, S. A., Logotheti, S., Mikas, D., Giarika, A., Gorgoulis, V., and Zoumpourlis, V. (2008) *BioEssays* **30,** 314–327
18. Yin, X., Dewille, J. W., and Hai, T. (2008) *Oncogene* **27,** 2118–2127
19. Chen, C., and Wells, A. D. (2007) *PLoS ONE* **2,** e912
20. Ying, T. H., Hsieh, Y. H., Hsieh, Y. S., and Liu, J. Y. (2008) *Cell Biol. Int.* **32,** 210–216
21. Wasylyk, C., Zheng, H., Castell, C., Debussche, L., Multon, M. C., and Wasylyk, B. (2008) *Cancer Res.* **68,** 1275–1283
22. Young, M. R., Li, J. J., Rincón, M., Flavell, R. A., Sathyanarayana, B. K., Hunziker, R., and Colburn, N. (1999) *Proc. Natl. Acad. Sci. U.S.A.* **96,** 9827–9832
23. Lu, H., and Huan, C. (2007) *Curr. Cancer Drug Targets* **7,** 343–353
24. Lee, E. J., Hyun, S. H., Chun, J., and Kang, S. S. (2007) *Biochem. Biophys. Res. Commun.* **358,** 783–788
25. Yaffe, M. B., and Smerdon, S. J. (2001) *Structure* **9,** R33–38
26. Bromberg, J. F., Horvath, C. M., Besser, D., Lathem, W. W., and Darnell, J. E., Jr. (1998) *Mol. Cell Biol.* **18,** 2553–2558